



# Hindered decays from a non-yrast four-quasiparticle isomer in

$^{164}\text{Er}$

T.P.D. Swan,<sup>1</sup> P.M. Walker,<sup>1,2,\*</sup> Zs. Podolyák,<sup>1</sup> M.W. Reed,<sup>1</sup>

G.D. Dracoulis,<sup>3</sup> G.J. Lane,<sup>3</sup> T. Kibédi,<sup>3</sup> and M.L. Smith<sup>3</sup>

<sup>1</sup>*Department of Physics, University of Surrey,  
Guildford, Surrey GU2 7XH, United Kingdom*

<sup>2</sup>*CERN, CH-1211 Geneva 23, Switzerland*

<sup>3</sup>*Department of Nuclear Physics, R.S.P.E.,  
Australian National University, Canberra ACT 0200, Australia*

(Dated: September 25, 2012)

## Abstract

The half-life of a  $K^\pi = 12^+$  isomer in  $^{164}\text{Er}$  has been measured to be 68(2) ns, and new decay pathways have been identified. These include highly  $K$ -forbidden  $\gamma$ -ray transitions directly to the ground-state rotational band, with reduced hindrance values that can be compared with those found for heavier nuclides. The new data support the interpretation that the level density is a key variable in determining  $K$ -forbidden transition rates.

PACS numbers: 21.10.-k, 23.20.Lv, 27.70.+q

Keywords: isomers, forbidden transitions

Phone: +44-1483-686807

Fax: +44-1483-686781

---

\*Electronic address: p.walker@surrey.ac.uk

## I. INTRODUCTION

Understanding the decay rates of long-lived excited nuclear states, or isomers, is important for a more general appreciation of nuclear stability, especially as the limits to nuclear binding are approached [1, 2]. Furthermore, long-term prospects for the external control of isomeric decays lead to the hope for novel energy-storage capabilities and perhaps the development of  $\gamma$ -ray lasers [1, 3, 4]. However, while isomers are well known in deformed nuclei, the theoretical modeling of their decay transition rates remains at a relatively early stage of development [5, 6].

In deformed nuclei, “ $K$  isomers” arise from the approximate conservation of the  $K$  quantum number, which represents the angular-momentum projection on the symmetry axis of the intrinsic shape [7]. Electromagnetic decays where the change in  $K$  value exceeds the transition multipolarity,  $\lambda$ , are called  $K$ -forbidden, with a degree of forbiddenness,  $\nu = \Delta K - \lambda$ . The hindrance per degree of  $K$ -forbiddenness, referred to as the reduced hindrance, can be evaluated as  $f_\nu = (T_{1/2}^\gamma/T_{1/2}^W)^{1/\nu}$ , where  $T_{1/2}^\gamma$  is the partial  $\gamma$ -ray half-life, and  $T_{1/2}^W$  is the corresponding Weisskopf single-particle estimate. Reduced-hindrance values typically fall in the range  $20 < f_\nu < 200$  for well deformed nuclei, with smaller values usually being associated with specific  $K$ -mixing mechanisms. Such mechanisms include [7] rotational (Coriolis) mixing; vibrational mixing and/or tunneling through axially asymmetric shapes; level-density effects; and chance near-degeneracies of states with the same  $I^\pi$  (where  $I$  is the total angular momentum) but different  $K$  values.

Coriolis mixing and a chance near-degeneracy in  $^{174}\text{Lu}$  have been analyzed in detail by Dracoulis et al. [8], and the proposed underlying random interactions justify, at least partially, the influence of level density found earlier [9]. Nevertheless, data covering a broader range of nuclei are needed to test the general applicability of these ideas. To date, well defined half-lives and decay properties for multi-quasiparticle, high- $K$  isomers, involving two or more broken nucleon pairs, have existed only for a small region of nuclei with  $70 \leq Z \leq 76$  and  $102 \leq N \leq 108$  [7, 10–13]. The best examples outside this region are  $^{254}_{102}\text{No}$  (which will be discussed later) where the decay properties remain to be confirmed [14, 15], and the present case of a  $T_{1/2} \geq 170$  ns isomer in  $^{164}_{68}\text{Er}$  [16]. We now report new measurements for  $^{164}\text{Er}$ .

## II. EXPERIMENTAL METHOD

Nuclei in the  $^{164}\text{Er}$  region were populated using  $^9\text{Be} + ^{160}\text{Gd}$  fusion evaporation reactions. Pulsed and chopped beams were provided by the 14UD tandem accelerator at the ANU Heavy Ion Accelerator Facility [17] at an energy of 57 MeV. This beam energy provided the greatest cross section for  $^{164}\text{Er}$  production through the  $^{160}\text{Gd}(^9\text{Be},5\text{n})$  reaction. A highly enriched ( $> 95\%$ )  $^{160}\text{Gd}$  target with an effective thickness of  $4.4 \text{ mg/cm}^2$  was placed at the centre of the Compton suppressed CAESAR array [18], consisting of 6 HPGe detectors at  $\pm 48^\circ$ ,  $\pm 97^\circ$  and  $\pm 147^\circ$  in the beam plane, and 3 larger HPGe detectors, out of plane at  $\pm 45^\circ$  and  $+135^\circ$ . The array includes 2 out-of-plane LEPS detectors at  $-90^\circ$  and  $-135^\circ$  for greater efficiency at low energies.

Chopped and bunched 1 ns beam pulses, with  $1.7 \mu\text{s}$  separation, were used to measure  $\gamma$ -ray events relative to the driving RF signal. These events were sorted into a variety of event matrices, the most important for the present study being a “time- $\gamma$ ” (time vs. energy) matrix, an “out-of-beam  $\gamma$ - $\gamma$ ” matrix, containing pairs of  $\gamma$ -ray events detected between beam pulses, that were themselves coincident within  $\pm 150 \text{ ns}$ , and an “early-delayed  $\gamma$ - $\gamma$ ” matrix where event pairs had time differences between 150 ns and 832 ns in order to identify correlated events across isomeric states. The usual in-beam  $\gamma$ - $\gamma$  coincidences were also studied. From these data, previously unknown isomers were discovered in several product nuclides, as reported elsewhere [19, 20]. Here we focus on the  $^{164}\text{Er}$  results. Although this was the nuclide with the largest reaction cross section, a complete analysis of all the products was necessary before the lowest-intensity  $\gamma$ -ray transitions could be reliably identified. We note that the cross section for  $^{164}\text{Er}$  was approximately 44% of the total, 1.5% of which decayed through the isomer at 3.4 MeV.

## III. RESULTS

Following earlier high-spin, fusion-evaporation studies [21–23], the  $K^\pi = 12^+$ , 3.4 MeV isomer in  $^{164}\text{Er}$  was first identified by Bark et al. [16], together with a rotational band built on it. The isomer was found to decay by a 554 keV  $\gamma$ -ray transition, with a half-life estimated to be  $\geq 170 \text{ ns}$ , using a coincidence window of  $\sim 150 \text{ ns}$ . We now determine that the principal decay is by a 555.0(1) keV transition, which establishes a half-life of 68(2) ns

from its decay curve, as illustrated in fig. 1, and several additional  $\gamma$ -ray transitions with consistent half-lives have been identified. A sample out-of-beam  $\gamma$ - $\gamma$ -coincidence spectrum is shown in fig. 2. From spectra such as this, and by building on previous work [16, 21–24], a detailed scheme has been constructed for the  $\gamma$ -ray decay of the  $K^\pi = 12^+$  isomer, as shown in fig. 3. The transition placements and relative intensities are listed in tables I and II. The lowest-intensity transitions now identified to depopulate the  $K^\pi = 12^+$  isomer are at 1295 keV and 1860 keV, the latter being tentatively placed. Both go directly to the ground-state band ( $g$ -band). Fig. 4 shows part of the coincidence spectrum gated by the 410 keV  $g$ -band transition. The placements are supported by other similar spectra.

Our new data confirm the tentative  $K^\pi = 12^+$  assignment of Bark et al. [16] for the 3378 keV isomer. A spin of at least  $12\hbar$  is implied by the absence of a transition from the isomer to the  $10^-$  member of the  $K^\pi = 7^-$  band, in competition with the intense 555 keV transition to the  $11^-$  band member. The intensity flow through the newly assigned 3222 keV level (see fig. 3 and tables I and II) then determines the 156 keV electron conversion coefficient to be  $\alpha_T = 0.12(11)$ , compared to theoretical values [25] of 0.10 for  $E1$  and 0.80 for  $M1$  transitions. This establishes  $E1$  character for the 156 keV transition, together with stretched-quadrupole character for the subsequent 462 and 774 keV transitions. In the absence of additional half-lives greater than 10 ns these are given  $E2$  assignments, resulting in  $I^\pi = 12^+$  for the isomer. No other assignments provide a consistent interpretation of the level structure. The usual assumption is made that  $K = I$  for the isomeric bandhead.

As shown on the right-hand side of fig. 3, two fragments of rotational bands are identified in the decay of the  $K^\pi = 12^+$  isomer. Negative parity is assigned to the left-hand fragment, on account of the decay path discussed above. In both fragments, out-of-band transitions to the known  $K^\pi = 7^-$  band compete with in-band transitions. The absence of well defined bandheads prevents specific  $K$ -value assignments, but high values ( $K = 7-9$ ) are implied by the evident lack of significant  $K$ -forbiddenness in the out-of-band transitions to the  $K^\pi = 7^-$  band (as well as the absence of branches to the known [24] lower- $K$  structures).

#### IV. DISCUSSION

Bark et al. [16], argued that the  $K^\pi = 12^+$  isomer can be assigned the four-quasiparticle  $2\pi \otimes 2\nu$  configuration  $\{\pi 7/2^- [523], \pi 7/2^+ [404], \nu 5/2^+ [642], \nu 5/2^- [523]\}$ , in which the  $2\pi$

component corresponds to the configuration of the  $K^\pi = 7^-$  isomer. The three well-established  $E1$  decays from the two isomers (see table I) are of comparable strength, with  $42 \leq f_\nu \leq 94$ , which is similar to the range of values found, for example, for the  $E1$  decays from the  $N = 106$ ,  $K^\pi = 8^-$  isomers [26]. Effective  $f_\nu$  values are also included in table I, where the Weisskopf hindrance factor,  $F_W$ , is first divided by  $10^4$  before evaluating the  $E1$  reduced hindrance [16]. This is a somewhat arbitrary division, in an attempt to allow for the typically hindered nature of  $K$ -allowed  $E1$  transitions. As shown in table I, these three  $f_\nu^{eff}$  values are very similar, ranging from 9.0 to 9.4.

It is notable that the  $M1$  transitions from the  $K^\pi = 7^-$  isomer are strongly hindered ( $F_W > 10^4$ ) despite being only one-fold forbidden ( $\nu = 1$ ). This is most likely a consequence of the populated states, with nominal  $K = 5$  assignments, being strongly mixed with lower- $K$  octupole-vibrational states. These mixings have been discussed by Fields et al. [23]. In addition to the octupole admixtures, the  $i_{13/2}$  neutron in the  $K^\pi = 5^-$ ,  $\{\nu 5/2^+[642], \nu 5/2^-[523]\}$  configuration is affected by Coriolis mixing which also introduces lower- $K$  components.

We now focus on the reduced-hindrance values of the highly  $K$ -forbidden  $E2$  and  $M1$  transitions,  $f_\nu = 5.9$  and  $6.2$  respectively, that connect the  $K^\pi = 12^+$  isomer to the  $g$ -band, as given in table I. These can be compared with decays from other similar isomers. The reduced hindrance, particularly for  $K$ -forbidden  $E2$  transitions from four- and five-quasiparticle isomers, has been found [9] to be inversely correlated with  $E - E_R$ , where  $E$  is the isomer excitation energy and  $E_R$  is the rigid-rotor energy at the same angular momentum. This was interpreted to be due to level-density effects, in the sense that more highly excited isomers (relative to a rigid rotor) suffer additional  $K$  mixing due to the increased density of states with the same  $I^\pi$  but different  $K$  values. Until now, this kind of analysis [9, 12, 27, 28] has been restricted to the mass region  $A = 174 - 184$ .

With a moment of inertia of  $74 \hbar^2 \text{MeV}^{-1}$  for  $^{164}\text{Er}$ , calculated by scaling with  $A^{5/3}$  from the value of  $85 \hbar^2 \text{MeV}^{-1}$  [9] for  $^{178}\text{Hf}$ , a rigid-rotor energy of 1052 keV is obtained for  $I = 12$ . This gives  $E - E_R = 2.326$  MeV for the  $K^\pi = 12^+$  isomer. Fig. 5 includes the reduced hindrance,  $f_\nu = 5.9$ , for the  $E2$  branch from the  $K^\pi = 12^+$ ,  $^{164}\text{Er}$  isomer, alongside other four- and five-quasiparticle isomers with known  $E2$  or  $E3$   $K$ -forbidden decays. The data point for the  $^{164}\text{Er}$  isomer agrees well with the general trend. It is notable that this single data point extends the mass range covered by the graph by a factor of two.

It is worthwhile to comment on the data points that fall well below the curve (i.e. the

level-density estimate) in fig. 5. As discussed previously [7, 9], the high- $K$  couplings of two  $i_{13/2}$  neutrons to form “ $t$ -bands” can lead to apparently low  $f_\nu$  values, when there is also  $g$ -band mixing. Such considerations can be difficult to take into account quantitatively, but seem to play a role in the low  $f_\nu$  values of, for example, the four-quasiparticle isomer decays of  $^{174}\text{Hf}$ ,  $^{176}\text{W}$  and  $^{182}\text{Os}$ . The fact there is little or no corresponding low- $f_\nu$  effect in the case of  $^{164}\text{Er}$  is consistent with this interpretation, since the neutron Fermi level is significantly lower in the  $i_{13/2}$  multiplet, i.e. close to the low- $\Omega$  orbitals, thus reducing the mean  $K$ -value of the  $t$ -band. However, there would be an increase in other Coriolis  $K$ -mixing effects, due to the proximity of the neutron Fermi level to the low- $\Omega$ ,  $i_{13/2}$  orbitals [29]. Dracoulis et al. [26] performed particle-rotor model calculations to better understand the influence of initial-state Coriolis mixing on  $K$ -forbidden  $E1$  decays in the  $N = 106$  isotones, for which the neutron Fermi level is close to the  $9/2^+[624]$ ,  $i_{13/2}$  orbital. Even without changing the neutron number, it is evident that differences in Coriolis mixing in the initial (isomeric) state can have a large effect on relative  $f_\nu$  values, and the “underlying” [26] reduced hindrance can be as much as ten times the observed value. It would be valuable to extend that approach to the  $E2$  decays considered here, covering a wider range of the  $i_{13/2}$  multiplet. In particular, for  $^{164}\text{Er}$  the neutron Fermi level is close to the  $5/2^+[642]$ ,  $i_{13/2}$  orbital, so that stronger Coriolis effects may be anticipated. Despite these considerations, a substantial  $f_\nu(E2)$  value is nevertheless found for the  $^{164}\text{Er}$  four-quasiparticle isomer decay, and this remains the case even if the intensity of the 1860 keV transition is treated as an upper limit, since it would then correspond to a lower limit in reduced hindrance.

The variation of the reduced hindrance of the  $\Delta I = 0$  decays (with  $M1$  multipolarity assumed) has been analysed by Swan [30]. There is more scatter of the data points, which could be related to the  $M1$  assumption and different  $E2/M1$  mixing ratios, but the  $^{164}\text{Er}$  data point remains in good accord with the other isomers. For example, the  $^{174}\text{Yb}$  value of  $f_\nu = 6.6$  [12] is close to the  $^{164}\text{Er}$  value of 6.2 (with similar  $E - E_R$  values, as evident from fig. 5).

Finally, we consider briefly the situation in the heaviest mass region where four-quasiparticle high- $K$  isomers have been identified. Although significantly different level structures have been proposed for  $^{254}\text{No}$  [14, 15], it is only the work of Clark et al. [15] that specifies the assignment and decay of a  $K^\pi = 16^+$  isomer at 2928 keV, also non-yrast, in sufficient detail for reduced-hindrance determination. With, tentatively,  $f_\nu = 24$  and

$E - E_R = 2043$  keV, the reduced hindrance of the assigned  $E2$  decay from the isomer is in remarkably good accord with the behavior discussed above for the  $A = 164 - 184$  region. If these data [15] can be verified, then, together with the new  $^{164}\text{Er}$  results, there is substantial support for the key role of level density in the decay rates of high- $K$ , four- and five-quasiparticle isomers. Limited data in the  $A = 180$  region for higher quasiparticle numbers are also in agreement with this conclusion [27].

In summary, the  $K^\pi = 12^+$  isomer in  $^{164}\text{Er}$  has been studied using pulsed-beam  $\gamma$ -ray spectroscopy. With improved sensitivity to isomeric decays, the half-life and decay radiations have been remeasured. The new half-life of  $T_{1/2} = 68(2)$  ns, together with a 0.3% branching ratio for the  $K$ -forbidden  $E2$  decay directly to the  $g$ -band, yields a reduced hindrance of  $f_\nu = 5.9_{-0.2}^{+0.4}$  for this transition, or  $f_\nu > 5.5$  at the  $2\sigma$  level in transition intensity. In conjunction with the excitation energy of the four-quasiparticle state, this result supports the suggested key role of level density in determining the decay rates of high- $K$ , multi-quasiparticle isomers, over an extended mass region.

We thank the Australian Research Council, UK STFC, and AWE plc for financial support.

- 
- [1] P.M. Walker and G.D. Dracoulis, *Nature (London)* **399**, 35 (1999).
- [2] F.R. Xu, E.G. Zhao, R. Wyss, and P.M. Walker, *Phys. Rev. Lett.* **92**, 252501 (2004).
- [3] G.C. Baldwin and J.C. Solem, *Rev. Mod. Phys.* **69**, 1085 (1997).
- [4] P.M. Walker and J.J. Carroll, *Physics Today* **58**, 39 (June 2005).
- [5] S. Frauendorf, *Rev. Mod. Phys.* **73**, 463 (2001).
- [6] F. Chen, Y. Sun, P.M. Walker, G.D. Dracoulis, Y.R. Shimizu, and J.A. Sheikh, to be published.
- [7] P.M. Walker and G.D. Dracoulis, *Hyp. Int.* **135**, 83 (2001).
- [8] G.D. Dracoulis, F.G. Kondev, G.J. Lane, A.P. Byrne, T.R. McGoram, T. Kibédi, I. Ahmad, M.P. Carpenter, R.V.F. Janssens, T. Lauritsen, C.J. Lister, D. Seweryniak, P. Chowdhury, and S.K. Tandel, *Phys. Rev. Lett.* **97**, 122501 (2006).
- [9] P.M. Walker, D.M. Cullen, C.S. Purry, D.E. Appelbe, A.P. Byrne, G.D. Dracoulis, T. Kibédi, F.G. Kondev, I.Y. Lee, A.O. Macchiavelli, A.T. Reed, P.H. Regan, and F. Xu, *Phys. Lett. B* **408**, 42 (1997).
- [10] T. Shizuma, K. Matsuura, Y. Toh, Y. Hayakawa, M. Oshima, Y. Hatsukawa, M. Matsuda, K. Furuno, Y. Sasaki, T. Komatsubara, and Y.R. Shimizu, *Nucl.Phys. A* **696**, 337 (2001).
- [11] T. Shizuma, P.D. Stevenson, P.M. Walker, Y. Toh, T. Hayakawa, M. Oshima, K. Furuno, and T. Komatsubara, *Phys. Rev. C* **65**, 064310 (2002).
- [12] G.D. Dracoulis, G.J. Lane, F.G. Kondev, A.P. Byrne, T. Kibédi, H. Watanabe, I. Ahmad, M.P. Carpenter, S.J. Freeman, R.V.F. Janssens, N.J. Hammond, T. Lauritsen, C.J. Lister, G. Mukherjee, D. Seweryniak, P. Chowdhury, and S.K. Tandel, *Phys.Rev. C* **71**, 044326 (2005); Erratum *Phys. Rev. C* **73**, 019901 (2006).
- [13] S.K. Tandel, P. Chowdhury, E.H. Seabury, I. Ahmad, M.P. Carpenter, S.M. Fischer, R.V.F. Janssens, T.L. Khoo, T. Lauritsen, C.J. Lister, D. Seweryniak, and Y.R. Shimizu, *Phys. Rev. C* **73**, 044306 (2006).
- [14] F.P. Hessberger, S. Antalic, B. Sulignano, D. Ackermann, S. Heinz, S. Hofmann, B. Kindler, J. Khuyagbaatar, I. Kojouharov, P. Kuusiniemi, M. Leino, B. Lommel, R. Mann, K. Nishio, A.G. Popeko, S. Saro, B. Streicher, J. Uusitalo, M. Venhart, and A.V. Yeremin, *Eur. Phys. J. A* **43**, 55 (2010).
- [15] R.M. Clark, K.E. Gregorich, J.S. Berryman, M.N. Ali, J.M. Allmond, C.W. Beausang, M.



- Cromaz, M.A. Deleplanque, I. Dragojevic, J. Dvorak, P.A. Ellison, P. Fallon, M.A. Garcia, J.M. Gates, S. Gros, H.B. Jeppesen, D. Kaji, I.Y. Lee, A.O. Macchiavelli, K. Morimoto, H. Nitsche, S. Paschalis, M. Petri, L. Stavsetra, F.S. Stephens, H. Watanabe, and M. Wiedeking, *Phys. Lett. B* **690**, 19 (2010).
- [16] R.A. Bark, P. Bosetti, G.B. Hagemann, H. Ryde, A. Brockstedt, H. Carlsson, L.P. Ekstrom, A. Nordlund, B. Herskind, S. Leoni, A. Bracco, F. Camera, S. Frattini, M. Mattiuzzi, B. Million, C. Rossi-Alvarez, G. de Angelis, D. Bazzacco, S. Lunardi, and M.De Poli, *Z. Phys. A* **359**, 5 (1997).
- [17] G.D. Dracoulis, *Nucl. Phys. News* **9**, 1 (1999).
- [18] G.D. Dracoulis and A.P. Byrne, ANU-P/1052(1995)115 (1995) unpublished.
- [19] T.P.D. Swan, P.M. Walker, Zs. Podolyák, M.W. Reed, G.D. Dracoulis, G.J. Lane, T. Kibédi, and M.L. Smith, *Phys. Rev. C* **83**, 034322 (2011).
- [20] T.P.D. Swan, P.M. Walker, Zs. Podolyák, M.W. Reed, G.D. Dracoulis, G.J. Lane, T. Kibédi, and M.L. Smith, *Phys. Rev. C* **85**, 024313 (2012).
- [21] O.C. Kistner, A.W. Sunyar, and E. der Mateosian, *Phys. Rev. C* **17**, 1417 (1978).
- [22] S.W. Yates, I.Y. Lee, N.R. Johnson, E. Eichler, L.L. Riedinger, M.W. Guidry, A.C. Kahler, D. Cline, R.S. Simon, P.A. Butler, P. Colombani, F.S. Stephens, R.M. Diamond, R.M. Ronningen, R.D. Hichwa, J.H. Hamilton, and E.L. Robinson, *Phys. Rev. C* **21**, 2366 (1980).
- [23] C.A. Fields, K.H. Hicks, R.A. Ristinen, F.W.N. De Boer, L.K. Peker, R.J. Peterson, and P.M. Walker, *Nuc. Phys. A* **422**, 215 (1984).
- [24] B. Singh, *Nucl. Data Sheets* **93**, 243 (2001).
- [25] T. Kibédi, T.W. Burrows, M.B. Trzhaskovskaya, P.M. Davidson, and C.W. Nestor, *Nucl. Instr. and Meth. A* **589**, 202 (2008).
- [26] G.D. Dracoulis, G.J. Lane, F.G. Kondev, H. Watanabe, D. Seweryniak, S. Zhu, M.P. Carpenter, C.J. Chiara, R.V.F. Janssens, T. Lauritsen, C.J. Lister, E.A. McCutchan, and I. Stefanescu, *Phys. Rev. C* **79**, 061303(R), (2009).
- [27] P.M. Walker, *Acta Phys. Pol. B* **36**, 1055 (2005).
- [28] P.M. Walker, *Int. J. Mod. Phys. E* **15**, 1637 (2006).
- [29] F.S. Stephens, *Rev. Mod. Phys.* **47**, 43 (1975).
- [30] T.P.D. Swan, PhD Thesis, University of Surrey (2010), unpublished

TABLE I: Gamma-ray energy, relative intensity, final angular momentum, multipolarity, total conversion coefficient, hindrance factor, forbiddenness, and reduced hindrance for direct branches from the  $K^\pi = 12^+$ , 3378 keV isomer (upper section) and the  $K^\pi = 7^-$ , 1985 keV isomer (lower section).

$E_\gamma(\text{keV})$	$I_\gamma$	$I_f^\pi(\sigma\lambda)$	$\alpha^T$	$F_W$	$\nu$	$f_\nu$	$f_\nu^{eff\ a)}$
156.4(1)	22 (2)	$11^-(E1)$	0.099	$8.0 \times 10^6$	$2-4^b)$	53-2800	5.3-28
427.3(1)	21 (1)	(11) $(E1)^c)$	0.008	$1.7 \times 10^8$	$2-4^b)$	114-13000	11-130
		(11) $(M1)^c)$	0.052	$1.7 \times 10^6$	$2-4^b)$	36-1300	
555.0(1)	100 (3)	$11^-(E1)$	0.004	$7.7 \times 10^7$	4	94(1)	9.4(1)
1294.8(3)	2.0 (3)	$12^+(M1)$	0.003	$5.0 \times 10^8$	11	6.2(1)	
1859.5(6)	0.4 (2)	$10^+(E2)$	0.001	$5.3 \times 10^7$	10	$5.9_{-0.2}^{+0.4}$	
139.8(1)	57 (2)	$7^-(M1)$	1.095	$1.9 \times 10^4$	1		
240.4(1)	181 (6)	$6^-(M1)$	0.242	$3.1 \times 10^4$	1		
960.6(2)	5.6 (7)	$8^+(E1)$	0.001	$6.1 \times 10^9$	6	43(1)	9.2(2)
1370.6(2)	19 (1)	$6^+(E1)$	0.001	$5.3 \times 10^9$	6	42(1)	9.0(2)

Notes: <sup>a)</sup> The effective reduced hindrance for an  $E1$  transition, with  $F^W$  divided by  $10^4$ .

<sup>b)</sup> The  $K$  value of the populated state is uncertain (see text).

<sup>c)</sup> Both  $E1$  and  $M1$  options are given for the 427.3 keV transition.

TABLE II: Gamma-ray energy, relative intensity, initial level energy, initial angular momentum and final angular momentum for the new band fragments identified in  $^{164}\text{Er}$ , ordered by level spin from highest to lowest. Top: follows the 156 keV isomeric transition. Bottom: follows the 427 keV isomeric transition. The uncertainty in the  $\gamma$ -ray energies is typically 0.1 keV.

$E_\gamma(\text{keV})$	$I_\gamma$	$E_i$	$I_i^\pi$	$I_f^\pi$
240.6	10 (1)	3222	$11^-$	$10^-$
462.3	1.6 (2)	3222	$11^-$	$9^-$
637.5	3.9 (4)	3222	$11^-$	$10^-$
857.5	7.1 (5)	3222	$11^-$	$9^-$
221.7	2.8 (6)	2981	$10^-$	$9^-$
616.9	1.2 (2)	2981	$10^-$	$9^-$
816.8	4.9 (5)	2981	$10^-$	$8^-$
595.1	0.7 (3)	2759	$9^-$	$8^-$
773.9	3.6 (5)	2759	$9^-$	$7^-$
220.7	7 (2)	2951	(11)	(10)
366.6	4.8 (7)	2951	(11)	$10^-$
424.4	7.4 (8)	2951	(11)	(9)
203.7	5.2 (3)	2730	(10)	(9)
389.6	1.9 (2)	2730	(10)	(8)
185.9	6 (1)	2526	(9)	(8)
362.1	6.2 (5)	2526	(9)	$8^-$
355.0	9.6 (5)	2340	(8)	$7^-$

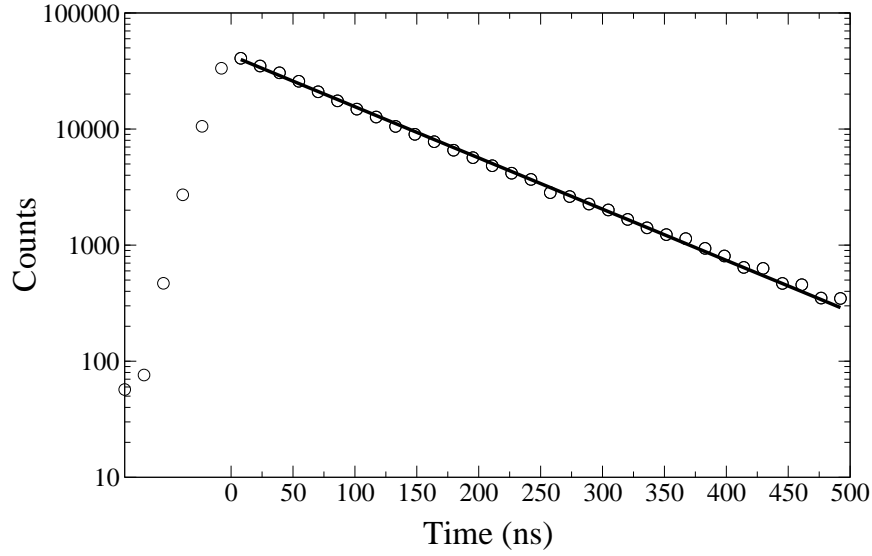


FIG. 1: Time spectrum for 555 keV  $\gamma$  rays. The fitted portion, shown by the solid line, gives a half-life of 68(2) ns.

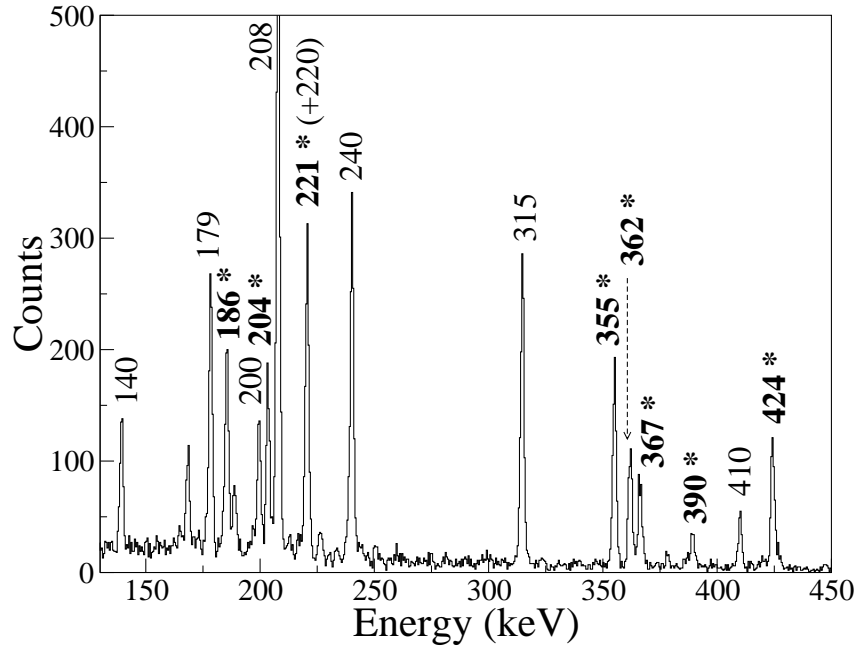


FIG. 2: Out-of-beam  $\gamma$ -ray spectrum in coincidence with 427 keV events. Newly placed transitions are indicated by asterisks. Other labeled transitions are known from previous studies. The unlabeled peaks at 169 and 189 keV are attributed to prompt break-through from above the  $K^\pi = 12^+$  isomer.

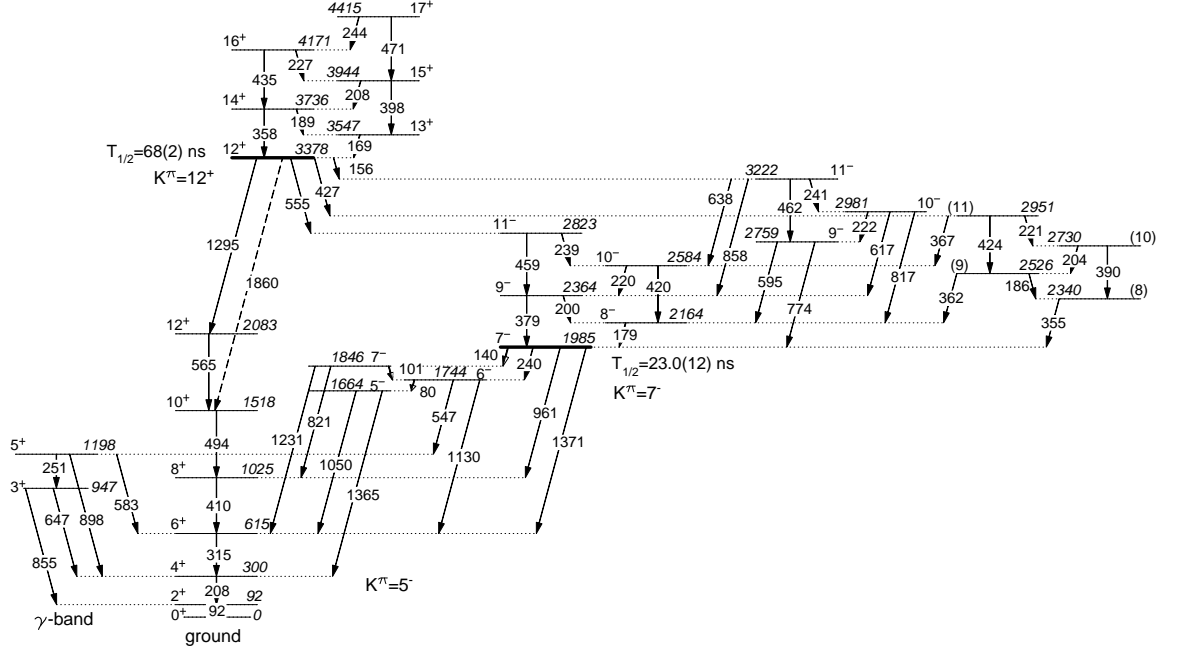


FIG. 3: Partial level scheme for  $^{164}\text{Er}$ , illustrating the decay pathways from the  $K^\pi = 12^+$ , four-quasiparticle isomer and the first few rotational excitations above the isomer. The dashed line for the 1860 keV transition indicates a tentative placement. Of the decay pathways from the  $K^\pi = 12^+$  isomer, only that through the 555 keV transition was previously known [16]. The half-life of the  $K^\pi = 7^-$  isomer is the adopted value from ref. [24].

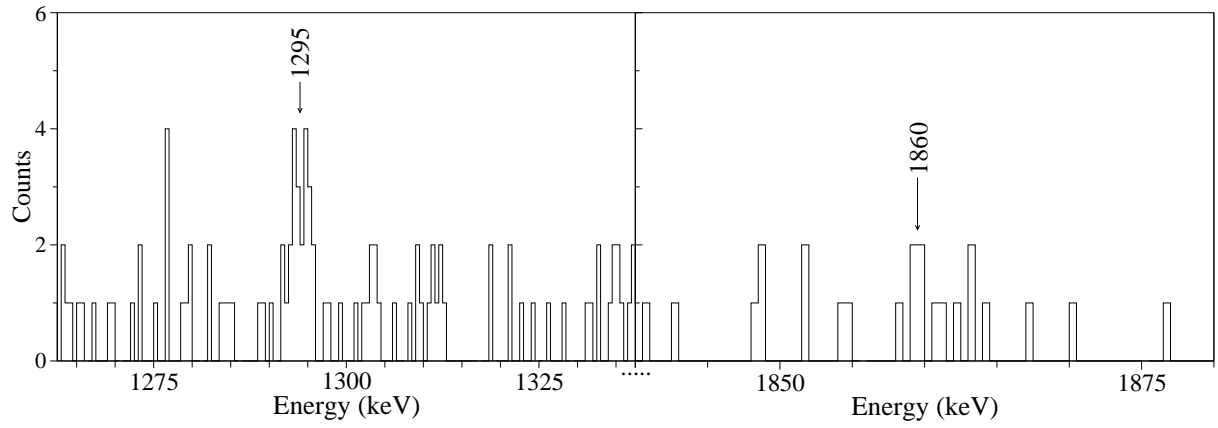


FIG. 4: Out-of-beam  $\gamma$ -ray spectrum in coincidence with 410 keV events. Newly placed transitions are indicated at 1295 and 1860 keV, the latter being tentative.

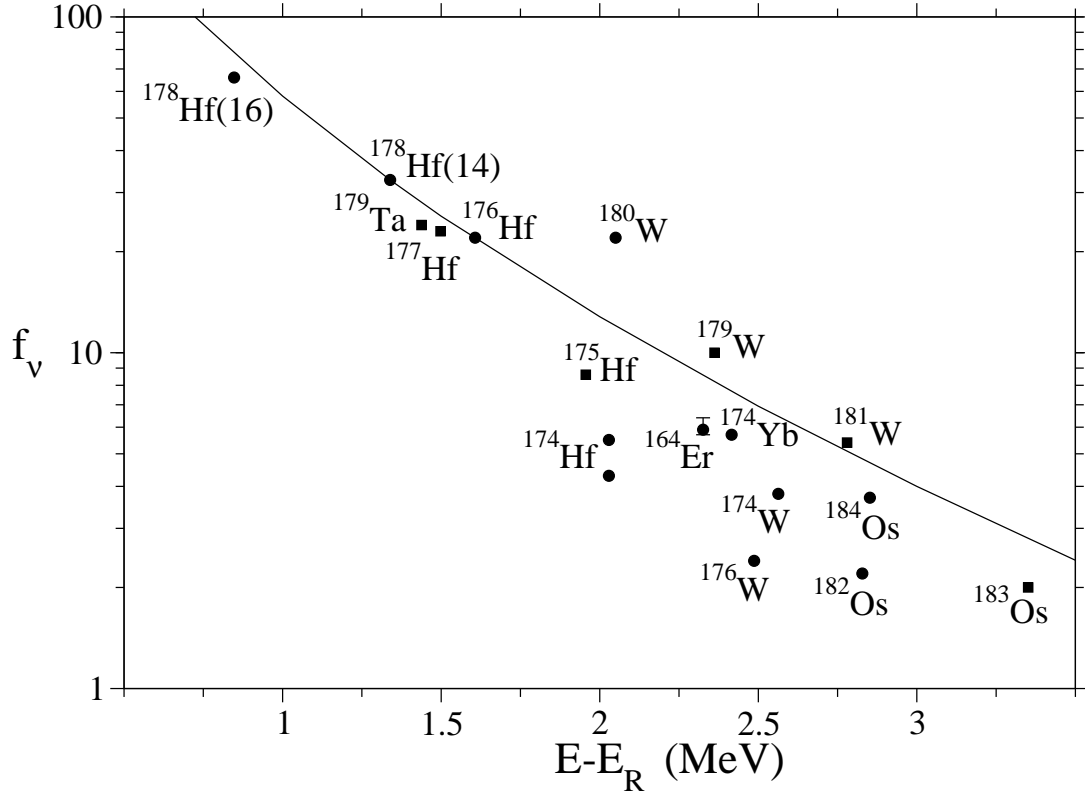


FIG. 5: Variation of  $E2$  and  $E3$  reduced-hindrance values with energy relative to a rigid rotor, for four- and five-quasiparticle,  $\Delta K > 5$  isomer decays (circles and squares, respectively) including the new  $^{164}\text{Er}$  value for the 1860 keV,  $E2$  transition, which, at the  $2\sigma$  level in transition intensity, corresponds to a lower limit in  $f_v$ . For odd- $A$  nuclides, a pairing energy of 0.9 MeV has been added. The curve represents a level-density estimate [9]. The data are from refs. [7, 10–13].